EASR

Engineering and Applied Science Research

https://www.tci-thaijo.org/index.php/easr/index

Published by the Faculty of Engineering, Khon Kaen University, Thailand

Combining accelerometry-based motion artifact cancellation with pulse oximetry processing

Theera Leeudomwong[1)], Tayard Deesudchit[2)] and Chedsada Chinrungrueng*[3)]

[1)]Biomedical Engineering Programme, Faculty of Engineering, Chulalongkorn University, Bangkok, Thailand
[2)]Division of Pediatric Neurology, Department of Pediatrics, Faculty of Medicine, Chulalongkorn University, Bangkok, Thailand
[3)]Department of Electrical Engineering, Faculty of Engineering, Chulalongkorn University, Bangkok, Thailand

Received 15 March 2017
Accepted 19 July 2017

Abstract

This paper proposes a combination of motion artifact (MA) cancellation with pulse oximetry processing. The objectives were to develop motion-resistant pulse oximetry processing relying on using accelerometry-based MA cancellation, and to explore the performance of the proposed processing method in providing arterial oxygen saturation ($\%SpO_2$) when the red and infrared (IR) photoplethysmogram (PPG) were corrupted by a MA. A PPG acquisition system was designed and constructed in the laboratory for the experiments. A three-axis accelerometer was utilized to detect the motion of a finger probe. An acceleration signal corresponding to the longitudinal direction of the finger was used to generate a motion reference signal for active noise cancellation using an adaptive filter. A Savitzky-Golay filter was applied to obtain the normalized first derivative of red and IR PPGs, and to generate a motion reference signal. The MA was eliminated from the normalized first derivative of red and IR PPGs using an adaptive filter, of which the adaptive algorithm was a recursive least square (RLS) method. The appropriate filter order was 16. After the MA cancellation, the normalized first derivative of the red and IR PPGs were expected to be free of MA, and they represented the arterial light absorption. The ratio of red to IR absorption (r_a) was computed and converted to the $\%SpO_2$ using the saturation equation obtained from the calibration. The experimental results showed that the theoretical concept for combining the accelerometry-based MA cancellation with the pulse oximetry processing was practical. The proposed processing method helped reduce the error of the $\%SpO_2$ measurement when a MA was present, and it had more resistance to MA than conventional pulse oximetry processing.

Keywords: Pulse oximetry, Motion artifact, Accelerometer, Adaptive filtering

1. Introduction

Pulse oximetry, a non-invasive optical technique for measuring arterial oxygen saturation ($\%SpO_2$), has been widely used for monitoring blood oxygen saturation for decades. Conventional pulse oximetry (CPO) relies on detecting the photoplethysmogram (PPG) using two wavelengths of light, approximately red and infrared (IR), and finding the light absorption due of arterial blood from the detected PPG. Theoretically, the ratio between red to IR absorption (r_a) relates to the $\%SpO_2$. A major problem of the CPO processing is motion artifacts (MA), which are unwanted signals originating from body movement. A pulse oximeter, which is an instrument using pulse oximetry to find the $\%SpO_2$, usually misinterpreted the MA as the PPG, leading to inaccurate readings, false desaturation alarms, and missed true desaturation alarms [1].

Over the years, there have been many attempts to reduce or eliminate the impact of the MA upon pulse oximetry processing. A solution is to design a filtering method for eliminating the MA from the detected PPG using various signal processing techniques. A major drawback of these techniques is the overlap of the frequency band between the MA and PPG. Among the signal processing techniques, adaptive filters are an effective tool for eliminating the in-band noise, and they have been widely explored for MA cancellation from PPGs. The performance of an adaptive filter depends on several factors. One important point is to select a noise reference signal that correlates with the MA corruption in the PPG, but does not correlate with the PPG. Some researchers tried to synthesize a noise reference signal from the detected red and IR PPGs [2-4]. Several others applied a signal detected from an accelerometer as the noise reference. The latter group demonstrated that a MA corrupted PPG measured from a ring PPG sensor can be recovered using an adaptive filter. The motion reference signal was an acceleration signal corresponding to motion in the longitudinal direction of the artery [5-7]. Also, elimination of the MA from the detected PPG helped reduce the error of the $\%SpO_2$ measurement at the forehead [8].

In this study, accelerometry-based MA cancellation was combined with pulse oximetry processing to eliminate the

*Corresponding author. Tel.: 6686 816 4900
Email address: chedsada.c@chula.ac.th
doi: 10.14456/easr.2018.13

MA from the normalized first derivative red and IR PPGs, before they were further processed to determine the $\%SpO_2$. Measurements were at the finger. The main objective was to develop motion-resistant pulse oximetry processing that relies on using accelerometry-based MA cancellation. The theoretical concept behind the measurement is provided, and the performance of the proposed processing method to determine the $\%SpO_2$ from the MA-corrupted PPG is also explored. Details of the proposed processing method and the experiments are provided in more detail below.

2. Materials and methods

2.1 The PPG model

The conventional PPG model, which generally appears in the context of CPO, is based on the Beer-Lambert Law under the assumption that the pulsatile component of the PPG resulted from light absorption by arterial blood consisting of only oxyhaemoglobin (HbO_2) and deoxyhaemoglobin (Hb). This model works well only when the PPG is not corrupted by a MA. A MA is presumably caused by multiple factors, such as the movement of sensor relative to skin, deformation of tissues due to external pressure, and changes of hemodynamics. These factors cause changes in the optical path length between the light source and detector, resulting in MA contamination of the PPG. In this study, the conventional PPG model was revised by adding a term describing the attenuation of light caused by motion. The revised model can be written as follows:

$$I^{\lambda}(t) = I_0^{\lambda} e^{-\left(\varepsilon_{HbO_2}^{\lambda}[HbO_2]_a + \varepsilon_{Hb}^{\lambda}[Hb]_a\right)L_a^{\lambda}(t)} e^{-A_{dc}^{\lambda}} e^{-\mu_{motion}^{\lambda} L_{motion}^{\lambda}(t)} + n(t) \quad (1)$$

where λ represents the wavelength of light, $I^{\lambda}(t)$ is the detected light intensity, I_0^{λ} is the light intensity emitted from the light source, $[HbO_2]_a$ and $[Hb]_a$ represent the concentration of HbO_2 and Hb in the arterial blood, $\varepsilon_{HbO_2}^{\lambda}$ and $\varepsilon_{Hb}^{\lambda}$ represent the extinction coefficient of HbO_2 and Hb, respectively. $L_a^{\lambda}(t)$ represents the optical path length of light in arterial blood. The notation, A_{dc}^{λ}, represents the constant light absorption due to non-pulsatile tissues, while μ_{motion}^{λ} and $L_{motion}^{\lambda}(t)$ represent the absorption coefficient of the non-pulsatile tissues and the optical path length in the non-pulsatile tissues that respectively vary during body movement. $n(t)$ represents additive ambient noise.

2.2 Proposed processing method

The block diagram of the proposed processing method is shown in Figure 1. The operation and description of each block is described below.

2.2.1 Proprocessing

The detected red and IR PPGs are considered to behave according to Equation (1). The main objective of preprocessing is to eliminate the additive ambient noise and MA outside of the frequency band of interest. A Savitzky-Golay (SG) filter [9] is proposed for use in this stage because it can be designed to provide both a smoothed PPG and its first derivative, which are required for normalization with the derivative method of the next step. Since the maximum human pulse is about 240 beats per minute (BPM) or approximately 4 Hz, the pass band frequency was set at 5 Hz covering the maximum pulse frequency. After preprocessing, the detected PPG signal can be mathematically described as follows:

$$I^{\lambda}(t) = I_0^{\lambda} e^{-\left(\varepsilon_{HbO_2}^{\lambda}[HbO_2]_a + \varepsilon_{Hb}^{\lambda}[Hb]_a\right)L_a^{\lambda}(t)} e^{-A_{dc}^{\lambda}} e^{-\mu_{motion}^{\lambda} L_{motion}^{\lambda}(t)} \quad (2)$$

2.2.2 Normalization

Normalization is a process to eliminate the light absorption of non-pulsatile tissues in parts that do not vary

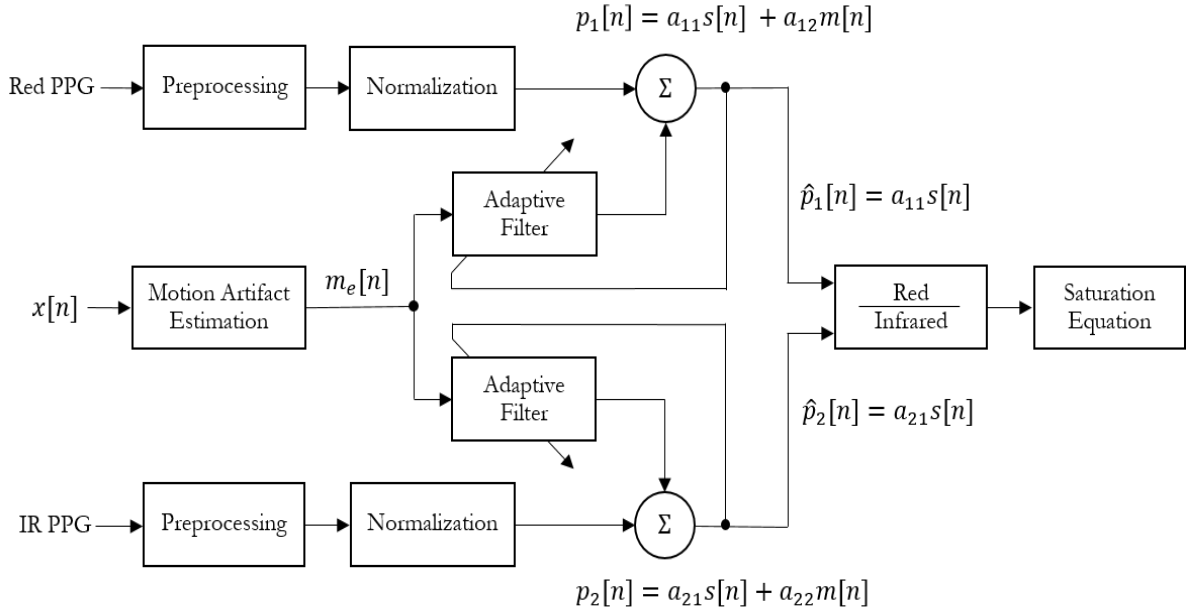

Figure 1 Block diagram of the proposed processing method

if there is motion, i.e. A_{dc}^{λ}. There are several ways to perform normalization, such as dividing by the maximum intensity, dividing by the average intensity, a logarithmic method, and a derivative method. In this study, the derivative method was chosen because of its simplicity. There is no need for additional algorithms, such as peak detection and/or interpolation to perform the normalization. Normalization using the derivative method provides a normalized first derivative as follows:

$$-\frac{(dI^{\lambda}(t)/dt)}{I^{\lambda}(t)} = \left(\varepsilon_{HbO_2}^{\lambda}[HbO_2]_a + \varepsilon_{Hb}^{\lambda}[Hb]_a\right)\frac{dL_a^{\lambda}(t)}{dt} + \mu_{motion}^{\lambda}\frac{dL_{motion}^{\lambda}(t)}{dt} \quad (3)$$

As seen in Equation (3), the normalization process transforms the MA from a multiplicative form into an additive form. When there is no motion, ($\frac{dL_{motion}^{\lambda}(t)}{dt} = 0$), the normalized first derivative PPG provides a term resulting from the arterial light absorption. When there is motion ($\frac{dL_{motion}^{\lambda}(t)}{dt} \neq 0$), it provides terms, which are a combination of the arterial light absorption and the MA.

Under the assumption that the variation of the optical path length is equal for both wavelengths, i.e., red and IR, the normalized first derivative of red and IR PPGs can be expressed as the discrete time signals as follows:

$$p_1[n] = a_{11}s[\mathrm{n}] + a_{12}m[n] \quad (4)$$

$$p_2[n] = a_{21}s[n] + a_{22}m[n] \quad (5)$$

where $p_1[n]$ and $p_2[\mathrm{n}]$ represent the normalized first derivative of the red and IR PPGs, $s[\mathrm{n}]$ and $m[\mathrm{n}]$ represent the first derivative of changes in the optical path length in the pulsatile and non-pulsatile tissues, a_{11} and a_{21} represent the absorption coefficients of the arterial blood at wavelengths λ_1 and λ_2, a_{12} and a_{22} represent the absorption coefficients of the non-pulsatile tissues, i.e., $\mu_{motion}^{\lambda_1}$ and $\mu_{motion}^{\lambda_2}$, respectively.

2.2.3 Motion artifact cancellation

An accelerometer and adaptive filter were utilized for eliminating the MA corruption in the normalized first derivative red and IR PPGs before they were further processed to determine the $\%SpO_2$. As shown in Figure 1, the primary input of the adaptive filter was applied to the normalized first derivative PPG corruption with the MA, while the reference input was applied by the MA reference signal ($m_e[n]$) obtained from the accelerometer.

It was agreed that the motion in the longitudinal direction of the finger, which is the same direction as the digital artery, causes a serious distortion of the PPG [5-7]. Using a single-axis acceleration signal from an accelerometer as the noise reference signal for noise cancellation was adequate to minimize the effect of MA corruption in the detected PPG [5-7, 10]. The MA reference signal used in this study was thus generated under the assumption that the variation of the acceleration signal in the longitudinal direction of the finger ($x[n]$) was proportional to the variation of the optical path length in the non-pulsatile tissues that varied during body movement, i.e., $L_{motion}^{\lambda}(t)$. From Equation (3), it can be seen that the MA is in the form of the first derivative of changes in the optical path length. Therefore, the MA reference signal, $m_e[n]$, can be obtained by taking the first derivative of $x[n]$, which can be written as:

$$m_e[n] = -(x[n] - x[n-1]) \quad (6)$$

2.2.4 Pulse oximetry processing

The main goal of pulse oximetry processing is to determine the $\%SpO_2$ by computing the ratio of the arterial light absorption between the red and IR (r_a) signals, which theoretically relates to the arterial oxygen saturation ($\%SpO_2$) as follows [11]:

$$\%SpO_2 = \frac{\left(\varepsilon_{Hb}^{\lambda_1} - \varepsilon_{Hb}^{\lambda_2}\right)r_a}{\varepsilon_{Hb}^{\lambda_1} - \varepsilon_{HbO_2}^{\lambda_2} + \left(\varepsilon_{HbO_2}^{\lambda_2} - \varepsilon_{Hb}^{\lambda_2}\right)r_a} \times 100 \quad (7)$$

In practice, this relationship is obtained from calibration.

After MA cancellation, the normalized first derivatives of the red and IR PPGs were expected to be free of the MA, and represented only the light absorption of the arterial blood as follows:

$$\hat{p}_1[n] = a_{11}s[n] \quad (8)$$

$$\hat{p}_2[n] = a_{21}s[n] \quad (9)$$

where $\hat{p}_1[n]$ and $\hat{p}_2[n]$ represent the normalized first derivative of red and IR PPG without MA, respectively. The ratio of the red to IR absorption (r_a) signals can be computed by analyzing a linear regression between the normalized first derivative of the red and IR PPGs as follows:

$$r_a = \frac{N\sum x_i y_i - \sum x_i \sum y_i}{N\sum x_i^2 - (\sum x_i)^2} \quad . \quad (10)$$

where x_i and y_i represent $\hat{p}_1[n]$ and $\hat{p}_2[n]$, respectively. N represents the number of samples, and i is the sample number. Finally, the ratio, r_a, was converted to the $\%SpO_2$ value using the saturation equation obtained from the calibration. The saturation equation used in this study is discussed in Section 3.1.

3. Experiments

3.1 The PPG acquisition system

A PPG acquisition system was designed and constructed for the experiments. It had two measurement channels (channels 1 and 2) so that measurements could be simultaneously performed at two different positions. Each channel can simultaneously detect both red and IR PPGs. Two commercial pulse oximeter finger probes were used. The wavelengths of light emitted from the light emitting diode (LED) inside each probe were measured using a spectrometer, USB4000-UV-VIS Ocean Optics. The peak wavelengths emitted from the first probe (probe 1) were 659 nm and 914 nm, and those emitted from the second probe (probe 2) were 659 nm and 920 nm. A 3-axis accelerometer was attached over probe 2 to detect the probe movement. The acceleration signal obtained was further used to generate a motion reference signal for the adaptive MA cancellation. All the detected signals were converted into a digital format using 12-bit analog-to-digital converters, and recorded on a personal computer and post-processed with MATLAB. The sampling frequency was 50 Hz.

A calibration was performed to derive the appropriate calibration curves for measuring the $\%SpO_2$ with each probe using a Fluke Biomedical $\%SpO_2$ Simulator Index 2. The calibration curve provided the relationship between the $\%SpO_2$ and the ratio, r_a, which is the ratio of the red absorption to IR absorption due to arterial blood. The $\%SpO_2$ defined at the simulator and the ratio, r_a, obtained from the measurement were fitted to a second-order polynomial. Equations (11) and (12) are the saturation equations appropriate for measuring $\%SpO_2$ with probes 1 and 2, respectively.

$$Probe\ 1: \quad \%SpO_2 = -22.97\ {r_a}^2 - 5.49\ r_a + 108.54 \tag{11}$$

$$Probe\ 2: \quad \%SpO_2 = -22.96\ {r_a}^2 - 4.76\ r_a + 108.22 \tag{12}$$

3.2 Measurement protocol

The developed PPG acquisition system was used to simultaneously detect the red and IR PPGs from a healthy human subject at two different positions. Probe 1, connected to channel 2, was clipped on the patient's left index finger, while the probe 2, attached to an accelerometer, was connected to channel 1 and clipped on the patient's right index finger. The measurement consisted of 2 protocols. For the first protocol, both fingers were stationary. The second protocol was divided into three states, resting, moving, and resting again. In the resting states, both fingers were stationary. In the moving stage, the left index finger remained stationary, while the right index finger performed a periodic finger bend synchronous with a metronome at various frequencies, 1, 2, and 3 Hz.

3.3 Signal processing

The red and IR PPGs, detected from both the left and right index fingers, were first preprocessed using a SG filter, of which the order and frame size of the SG filter were set at 2 and 11, respectively, to obtain a pass band frequency 5 Hz. Then, all signals were normalized using their derivatives. After normalization, CPO processing was used to find the ratio, r_a, and the $\%SpO_2$. The normalized first derivatives of the red and IR PPGs were segmented into time windows. Each window had a six second interval and was updated by shifting the window along the time axis every second, resulting in an overlap of five seconds. All windows were processed to find the r_a ratio using linear regression analysis according to Equation (10). The r_a ratio was then converted to $\%SpO_2$ using Equation (11) or (12), depending on the probe used.

The proposed processing method was only applied to the PPG detected from the right index finger. The motion reference signal according to Equation (6) was generated using the SG filter. Two adaptive algorithms, the least mean square (LMS) and the recursive least square (RLS), were tested for the MA cancellation. When the LMS was used, the step size was set constant at 0.004. When the RLS was used, the forgetting factor and the inverse correlation matrix were initially set to 0.99, and 1.0, respectively. The filter order was varied at levels of 2, 4, 16, 32, and 64. After the MA cancellation, the normalized first derivatives of the red and IR PPGs were segmented into time windows. In each window, the r_a ratio was computed using Equation (10), and converted to $\%SpO_2$ using Equation (12).

3.4 Performance evaluation

The performance of the proposed processing method was evaluated by comparing the $\%SpO_2$ obtained from the proposed processing method with the reference. As the left index finger was stationary in all measurement protocols, the $\%SpO_2$ measured at the left index finger employing CPO processing was used as a reference.

The root mean square error (RMSE) and Bland-Altman analysis were used for performance evaluation of the proposed processing method. The root mean square error (RMSE) was defined as:

$$RMSE = \sqrt{\frac{1}{N}\sum_{i=1}^{N}(y_i - \hat{y}_i)^2} \tag{13}$$

where y_i represents the $\%SpO_2$ obtained from the proposed processing method, $\hat{y}_i$ represents the reference $\%SpO_2$, N is the number of samples, and i is the sample number.

Bland-Altman analysis [12], which is a statistical method for comparing two different measurement techniques, was used to compare the $\%SpO_2$ measured from two different positions and methods. Bias is defined as the mean difference between the two methods ($\bar{d}$). Precision is the standard deviation (s) of differences, and the limits of agreement (LOA) indicating the boundary of the 95% confidence interval, $\bar{d} \pm 1.96s$. An LOA of less than $\pm 3\%$ is considered to be clinically acceptable [13].

4. Results and discussion

The $\%SpO_2$ data, obtained from using the proposed processing method, were collected during resting periods for 500 samples, and during periodic movement at 1 Hz, 2 Hz, and 3 Hz, for each with 110 samples. Figure 2 indicates the sum of RMSE resulting from using different adaptive algorithms and filter orders. It can be noted that the RLS algorithm provided a lower RMSE than the LMS algorithm, implying that the RLS algorithm was more resistant to MA than the LMS algorithm. The lowest RMSE occurred when the filter order was 16.

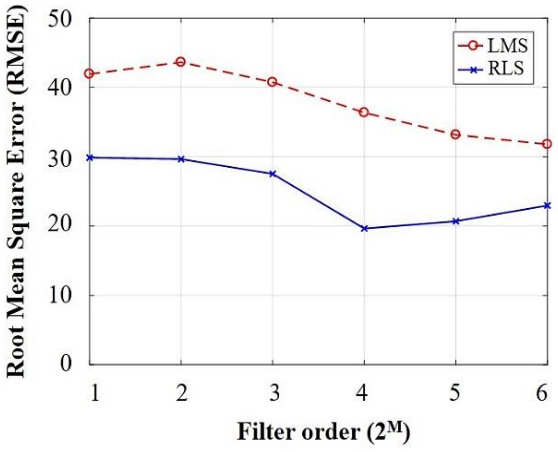

Figure 2 The sum of RMSE obtained using different adaptive algorithms and filter orders

Figure 3 shows a result of the $\%SpO_2$ measurement at two different positions and methods, when there was no MA. Figure 3a indicates that the $\%SpO_2$ measured at the right index finger using the proposed processing method was quite close to that measured at the left index finger using CPO processing. As shown in Figure 3b, Bland-Altman analysis revealed that the $\%SpO_2$ measured at the right index finger using the proposed processing method tended be a bit higher than that measured at the left index finger using the CPO processing. There were 500 samples (n) of analyzed data. The bias was 0.17 and the range of LOA was between -0.45 and 0.79. It can be interpreted that when there was no MA, the $\%SpO_2$ measured from both positions and methods was not clinically different.

Figure 4 shows an example of results of the $\%SpO_2$ measurement at two different positions and methods, when an MA was induced by periodic finger bending at 3 Hz. Figures 4a and 4b show the normalized first derivatives red and IR PPGs measured from the left and the right index fingers, respectively. During the measurements, the left index finger was stationary while the right index finger was moved by performing periodic finger bending. As shown in Figure 4c, when there was a MA induced by periodic finger bending, CPO processing provided a false desaturation, while the proposed processing method was still able to provide a $\%SpO_2$ value close to the reference.

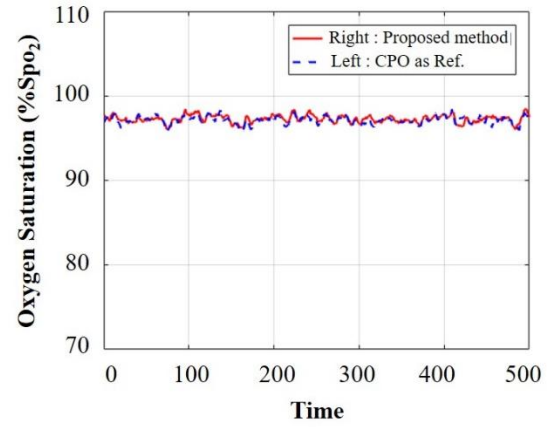

a) $\%SpO_2$ measured from the right index finger using the proposed processing method and that from the left index finger using the CPO when there was no MA.

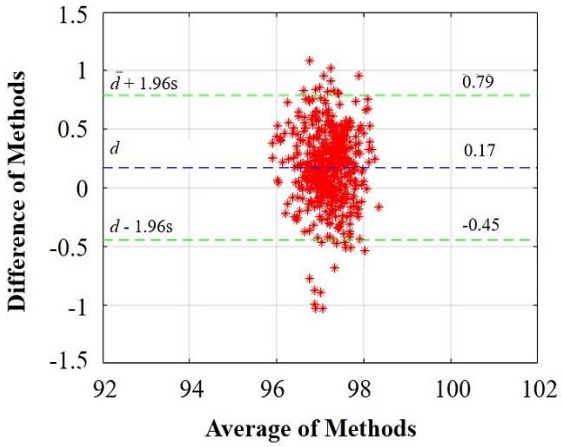

b) Bland–Altman plot

Figure 3 Results of the $\%SpO_2$ measurement at different positions and methods when there was no MA.

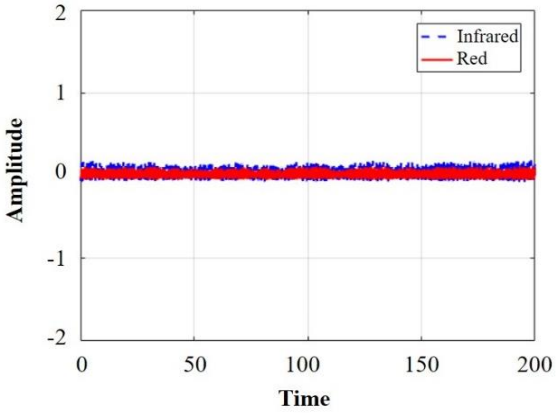

a) The normalized first derivative of the red and IR PPGs measured from the left index finger.

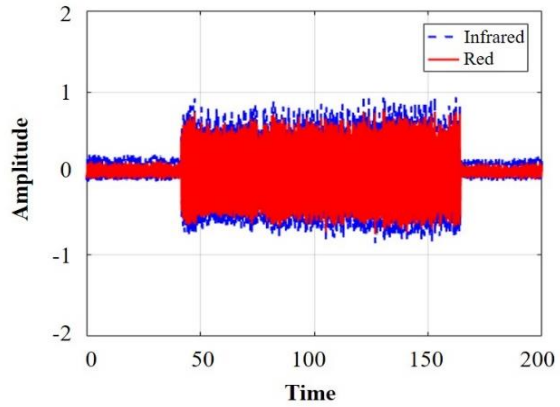

b) The normalized first derivative of red and IR PPGs measured from the right index finger.

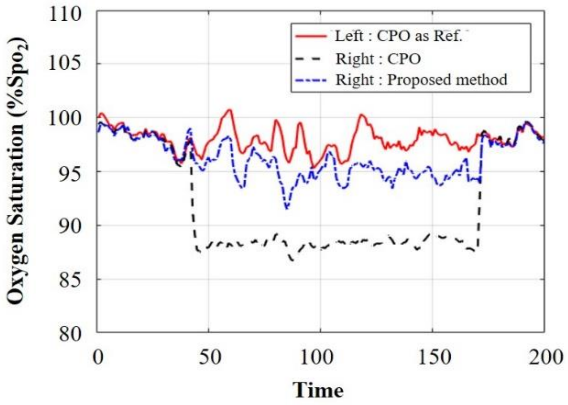

c) The comparison between the $\%SpO_2$ measured from the left and right index fingers.

Figure 4 Example of the $\%SpO_2$ measurement when there was a MA induced by periodic finger bending at 3 Hz.

Table 1 shows the Bland-Altman analysis of the $\%SpO_2$ measured from the right index finger without MA cancellation versus that from the left index finger. There were 110 samples (n) of analyzed data. When there was no MA, the $\%SpO_2$ measured from these positions were not significantly different. The bias was only 0.17%, and well within the range of LOA (-0.37% to 0.71%). However, when there was MA induced by periodic bending of the right index finger, it was noticed that the pulse

Table 1 Bland–Altman analysis between the $\%SpO_2$ measured from the right index finger without MA cancellation versus that from the left index finger (n = 110).

	Ch 1 without MA cancellation vs Ch 2 (as ref.)			
	no MA	**1 Hz**	**2 Hz**	**3 Hz**
Bias ($\bar{d}$)	0.17	-17.91	-13.30	-9.53
Precision (s)	0.28	1.60	1.17	1.20
+ LOA ($\bar{d} + 1.96s$)	0.71	-14.77	-11.00	-7.17
- LOA ($\bar{d} - 1.96s$)	-0.37	-21.04	-15.59	-11.89

Table 2 The Bland–Altman analysis between the $\%SpO_2$ measured from the right index finger with MA cancellation versus that from the left index finger (n = 110).

	Ch 1 with MA cancellation vs Ch 2 (as ref.)			
	no MA	**1 Hz**	**2 Hz**	**3 Hz**
Bias ($\bar{d}$)	0.17	-3.09	-2.36	-2.80
Precision (s)	0.32	1.13	1.76	1.19
+ LOA ($\bar{d} + 1.96s$)	0.79	-0.88	1.09	-0.47
- LOA ($\bar{d} - 1.96s$)	-0.45	-5.31	-5.82	-5.13

oximetry could be processed without MA cancellation, which is CPO processing, providing false desaturation. The bias was 17.91%, -13.30%, and -9.53%, corresponding to the frequency of periodic finger bending of 1, 2 and 3 Hz, respectively.

Table 2 shows the Bland-Altman analysis of the $\%SpO_2$ measured from the right index finger with MA cancellation versus that from the left index finger. Similarly, when there was no MA, the $\%SpO_2$ measured from both positions and methods were no significantly different. The bias was 0.17%, and well within the range of LOA (-0.45% to 0.79%). When there was MA corruption in the detected PPG, the bias was reduced to -3.09%, -2.36%, and -2.80%, corresponding to the frequency of periodic finger bending at 1, 2 and 3 Hz, respectively. It was indicated that the proposed processing method was more resistant to MA than CPO processing. However, the LOA was a bit wider than the clinically acceptable range.

The experimental results showed that CPO processing is highly sensitive to MA. It gave false desaturation when the detected red and IR PPGs were corrupted with a MA. The error of the $\%SpO_2$ measurement obtained using CPO processing was related to the frequency of the MA modulated in the detected PPG. The closer the MA frequency was to the pulse frequency, the higher the resulting error.

The theoretical concept for combining accelerometry-based MA cancellation and pulse oximetry processing proposed in this study is practical. The results show that the proposed processing method provided similar results to CPO processing when there was no MA, but it showed lower error than CPO processing when there was MA corruption in the PPG. Therefore, the proposed processing method has more resistance to MA than CPO processing. The factors affecting the performance of the proposed processing method were the adaptive algorithm, filter order, and noise in the reference signal. Among the adaptive algorithms, the RLS algorithm was the most effective for accelerometry-based MA cancellation. It was observed that a higher filter order provided the lower error, but an excessive filter order tended to result in slightly higher errors. The appropriate filter order was 16. It was reasonable to assume that the variation of the acceleration signal corresponding to the motion in longitudinal direction of the finger was proportional to the variation of the optical path length in the non-pulsatile tissues when they move. The MA reference signal proposed in Equation (6) was suitable to serve as a reference signal for the adaptive filter to eliminate the MA from the normalized first derivative PPG. Using a single acceleration signal from the accelerometer to generate the MA reference signal was shown to be adequate to minimize the MA corruption in the finger PPG.

As the LOA was still wider than the acceptable range, it was expected that the performance of the proposed processing method was limited by the signal-to-noise ratio (SNR) of the detected PPG. The periodic finger bend was a method that induces highly intense MA to the PPG. When the SNR was low, the MA could be partially eliminated from the MA corrupted PPG. Therefore, the effect of the MA upon pulse oximetry processing still remained. If the strength of the MA was lower, the LOA would be narrower and lie in the clinically acceptable range. We suggest combining accelerometry-based MA cancelation with the motion resistant pulse oximetry processing to further improve the performance of pulse oximetry processing.

5. Conclusion

MAs are a serious problem of pulse oximetry processing. In this study, accelerometry-based MA cancellation was combined with pulse oximetry processing to eliminate the MAs from the normalized first derivative of the red and IR PPGs before they were further processed to determine the $\%SpO_2$. The results revealed that the proposed processing method helped reduce the error of the $\%SpO_2$ measurement in the presence of a MA. It is expected that the performance of pulse oximetry processing would be further improved if the motion-resistant pulse oximetry processing were combined with accelerometry-based MA cancellation instead of the conventional pulse oximetry processing.

6. References

[1] Petterson MT, Begnoche VL, Graybeal JM. The effect of motion on pulse oximetry and its clinical significance. Anesth Analg. 2007;105(6 Suppl):S78-84.

[2] Ram MR, Madhav KV, Krishna EH, Komalla NR, Reddy KA. A novel approach for motion artifact reduction in PPG signals based on AS-LMS adaptive filter. IEEE Trans Instrum Meas. 2012;61(5):1445-57.

[3] Peng F, Zhang Z, Gou X, Liu H, Wang W. Motion artifact removal from photoplethysmographic signals by combining temporally constrained independent component analysis and adaptive filter. Biomed Eng Online. 2014;13:1-14.
[4] Yousefi R, Nourani M, Ostadabbas S, Panahi I. A motion-tolerant adaptive algorithm for wearable photoplethysmographic biosensors. IEEE J Biomed Health Informat. 2014;18(2):670-81.
[5] Asada HH, Hong-Hui J, Gibbs P. Active noise cancellation using MEMS accelerometers for motion-tolerant wearable bio-sensors. The 26th Annual International Conference of the IEEE Engineering in Medicine and Biology Society; 2004 Sep 1-5; San Francisco, USA. USA: IEEE; 2004. p. 2157-60.
[6] Gibbs P, Asada HH. Reducing motion artifact in wearable bio-sensors using MEMS accelerometers for active noise cancellation. Proceedings of the 2005 American Control Conference; 2005 Jun 8-10; Portland, USA. USA: IEEE; 2005. p. 1581-6.
[7] Wood LB, Asada HH. Noise cancellation model validation for reduced motion artifact wearable PPG sensors using MEMS accelerometers. 2006 International Conference of the IEEE Engineering in Medicine and Biology Society; 2006 Aug 30 - Sep 3; New York, USA. USA: IEEE; 2006. p. 3525-8.
[8] Comtois G, Mendelson Y, Ramuka P. A comparative evaluation of adaptive noise cancellation algorithms for minimizing motion artifacts in a forehead-mounted wearable pulse oximeter. Conference proceedings : Annual International Conference of the IEEE Engineering in Medicine and Biology Society IEEE Engineering in Medicine and Biology Society Annual Conference. 2007;2007:1528-31.
[9] Schafer RW. What is a Savitzky-Golay filter? [Lecture Notes]. IEEE Signal Process Mag. 2011;28(4):111-7.
[10] Relente AR, Sison LG. Characterization and adaptive filtering of motion artifacts in pulse oximetry using accelerometers. Proceedings of the Second Joint 24th Annual Conference and the Annual Fall Meeting of the Biomedical Engineering Society/Engineering in Medicine and Biology; 2002 Oct 23-26; Houston, USA. USA: IEEE; 2002. p. 1769-70.
[11] Wieben O. Light absorbance in pulse oximetry. In: Webster JG, editor. Design of pulse oximeters. Philadelphia: Institute of Physics Publishing; 1997.
[12] Bland JM, Altman DG. Statistical methods for assessing agreement between two methods of clinical measurement. Lancet. 1986;1(8476):307-10.
[13] Tungjitkusolmun S. Accuracy and errors. In: Webster JG, editor. Design of pulse oximeters. Philadelphia: Institute of Physics Publishing; 1997.